Astronomical and Astrophysical Transactions (*AApTr*), 2016, Vol. 29, Issue 2, pp. 129–142,
ISSN 1055-6796, Photocopying permitted by license only, ©Cambridge Scientific Publishers

Light produced by shocks and shocks produced by light: superluminous supernovae and GRB afterglows

S.I. Blinnikov[1,2,3,4,*]

[1]*Institute for Theoretical and Experimental Physics, NIC Kurchatov Institute, Moscow 117218, Russia*
[2]*Sternberg Astronomical Institute, Lomonosov Moscow State University, 13 Universitetsky pr., Moscow 119992, Russia*
[3]*All-Russia Research Institute of Automatics, Moscow 127055, Russia*
[4]*Kavli Institute for the Physics and Mathematics of the Universe, Kashiwa 277-8583, Japan*

Received 1 November, 2015

A shock wave which runs through rather dense matter surrounding an exploding star can produce enough light to explain many Superluminous Supernova events. On the other hand some 'bumps' in the light curves of GRB afterglows may be caused by reprocessing of powerful GRB light in non-uniformities of material around the GRB engine. The powerful photon flux may induce also some shocks in this medium.

Keywords: Supernovae; GRB afterglows; shock waves

1 Introduction

The mechanism of the explosion of recently discovered Superluminous supernovae (SLSN), which are extremely powerful and long lasting events, is still not fully understood. To explain observations (Fig. 1) one can consider either an unusually energetic explosion with a huge amount of ^{56}Ni produced, or an additional energy source like a millisecond 'magnetar' that somehow transforms its rotation energy into the energy of the SN ejecta, or an interaction of the ejecta with extended and dense circumstellar matter (CSM). I will concentrate on the latter option, namely shock-interaction models.

The idea of producing large radiative flux during the interaction of the gas ejected in two subsequent explosions was suggested by Grasberg & Nadyozhin (1986) for explanation of SNe IIn. One physical mechanism for those multiple explosions (pulsational pair instability, hence PPISN) was proposed by Heger & Woosley (2002), but

*Email: sblinnikov@gmail.com

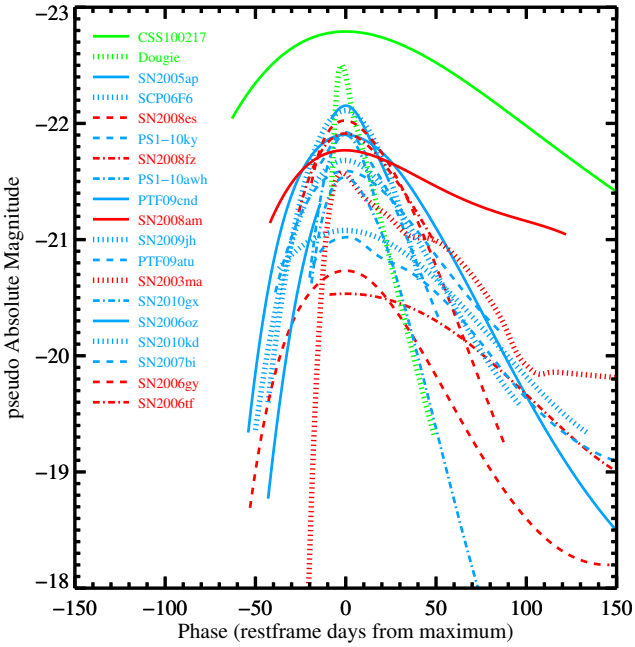


Figure 1 SLSNe luminosities in wide range (Quimby et al., 2013). Now SN2006gy, which was the most powerful superluminous supernova in 2006, is in the lower part of the set.

other ways to produce a dense cloud around a presupernova are plausible (see e.g., Barkov & Komissarov, 2011; Chevalier, 2012). Woosley et al. (2007) used the model of PPISN to explain Type II superluminous SN 2006gy as a moderately energetic explosion ($\sim 3 \cdot 10^{51}$ ergs) without any radioactive material.

2 Presupernova models

All presupernova models for this work have been constructed in the same way as we described in many papers (Chugai et al., 2004; Baklanov et al., 2005). A quasi-polytropic structure in mechanical equilibrium is considered in the interior part which we call "ejecta". The temperature is related to the density as $T \propto \rho^{0.31}$. This part has mass $M_{\rm ej}$ and radius $R_{\rm ej}$, which we have always taken to be equal to 10 $R_\odot$ in this work. $M_{\rm ej}$ can be much less than the total mass of the collapsing core and the condition of mechanical equilibrium is not necessary; it is just a convenient form of parametrization of models.

To make an interacting model we surround the ejecta by a rather dense envelope with the mass $M_{\rm w}$ extended to the radius $R_{\rm w}$. For all our models the outer radius of the envelope is about 10^5 $R_\odot$, or $\sim 7 \cdot 10^{15}$ cm. For most of the models the envelope has power-law density distribution $\rho \propto r^{-p}$, which simulates the envelope or the wind that surrounds the exploding star. For a steady wind, $p = 2$, but in the very last stages of the evolution of a presupernova star the wind may not be steady. For our models

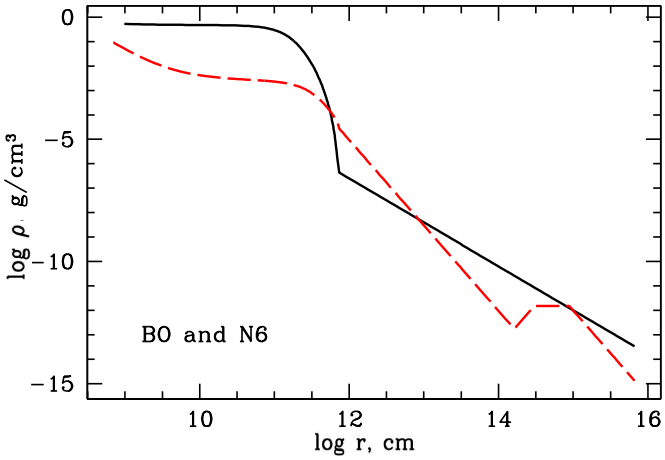


Figure 2 Two typical examples of the initial density structures for our models. The *solid* line shows windy-like model B0 (with broad light curve) with the total mass 54 $M_\odot$. The *dashed* line shows the model N6 (narrow light curve) with a detached shell; the total mass of the model is 10 $M_\odot$. The central part, which we call "ejecta", has a polytropic structure for all initial models.

we vary p in the range between 1.5 and 3.5. We tried also another kind of density distribution in outer layers: we construct a model with the envelope concentrated within a shell detached from the ejecta by a region of lower density. The density falls down and rises up still with power-low behaviour, but slopes of its distribution for this kind of models are steeper than in the windy-like models we described above. The density distributions for a couple of typical models are shown in Figure 2. No attempt is made to keep equilibrium in the envelope, but its dynamical time scale is so large that no appreciable motion has developed during the time of light curve simulation.

We calculate light curves for SNe exploding within these envelopes. A shock wave forms at the border between the ejecta and the envelope. It very efficiently converts the energy of the ordered motion of expanding gas to that of the chaotic thermal motion of particles, which can be easily emitted. As a result, we expect to derive light curves bright enough to explain at least a part of superluminous SNe I without an assumption of unusually high explosion energy.

Chemical elements in our models are distributed uniformly. Typically we use carbon-oxygen models with different C to O ratios or helium models.

3 Modelling with the STELLA code

The STELLA code, developed by us for supernova light curve simulations (Blinnikov et al., 1998, 2006), was employed for producing light curves to SLSNe in shock-interaction scenario. The main features of the code:

- multigroup time dependent radiation hydrodynamics;
- Non-relativistic ($O(v/c)$), spherically symmetric;

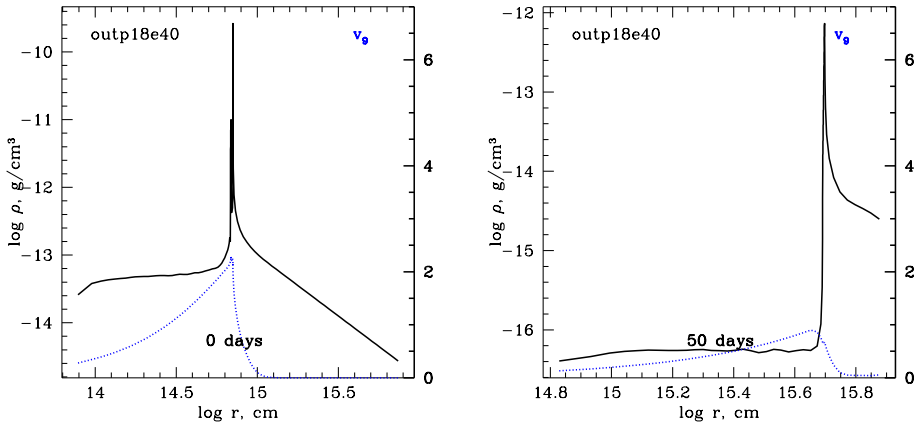


Figure 3 Long living dense shells from simulations described in (Sorokina et al., 2015). The decrease of velocity v is clear from the plots (blue lines, the scale is on the right Y-axis in units 10^9 cm/s). The kinetic energy of ejecta and shocked CSM is transformed into radiation which manifests itself as a SLSN.

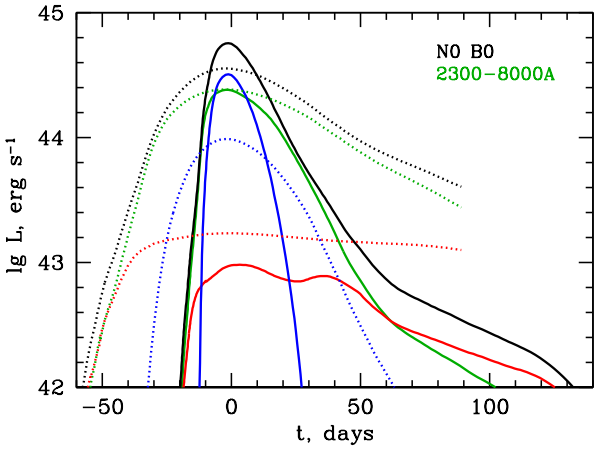


Figure 4 Bolometric light curves for the models with narrow light curves, N0 solid lines, and broad ones, B0 dotted lines.

- Lagrangian coordinates, staggered mesh;
- Full implicit time-dependent predictor–corrector solver for stiff ODE systems, modified Gear method (Brayton, Gustavson, Hatchel, 1972), see also Stabrowski (1997), flexible dynamic step and error control.

Our simulations (Sorokina et al., 2015) allow us to reproduce the wide range of LSNe in one class of models with modest energy, the shock-interaction model, which is the most economical option among other proposed scenarios (if one compares the energy budgets), see Fig. 4.

Bolometric light curves for the models with narrow light curves, N0 solid lines, and broad ones, B0 dotted lines. Black lines are true bolometrics. They show the light

curves integrated over the whole spectral range used in our calculation (1–50 000 Å). Black line is a sum of blue, green, and red lines which represent the parts of the total flux emitted in the extreme ultraviolet, visual, and far infrared ranges, respectively, but the borders between those ranges are different for the solid and dotted curves. The integration ranges for the visible (green) curves are written in the plots. The range 3250–8900 Å corresponds to the standard *UBVRI* range, while 2300–8000 Å, to the typical observed rest frame spectral range for SLSNe I whose redshift is usually pretty large.

The paper by Sorokina et al. (2015) contains many details on different models for SLSNe. Here I point out a few interesting results, not all of them are described in that paper.

Models for SN2010gx

Synthetic light curves for the model N0, one of the best for SN 2010gx, in r, g, B, and u filters compared with Pan-STARRS and PTF observations. Pan-STARRS points are designated with open squares (u, g, and R bands), PTF points, with filled circles (B and r bands). Four pink points in the beginning of the r band shows PTF observations in the Mould R-band which is similar to the SDSS r band.

Figure 7 presents rest frame observed (*red*) and modelled (*black*) spectra. On the left panel we compare the observed spectrum of SN 2010gx at day +27 (Quimby et al., 2013) with that of model N0 at day +32 after the maximum in B-band. The observed luminosities are in arbitrary units and can be shifted along y-axis for better fitting to the model. The right panel of Fig. 7 shows the observed spectrum of PTF09cnd at day −20 (Quimby et al., 2013) compared with the computed continuum spectrum of model B0 at day −20. The general agreement of the shapes of the observed and simulated spectra speaks in favour of correctness of our models.

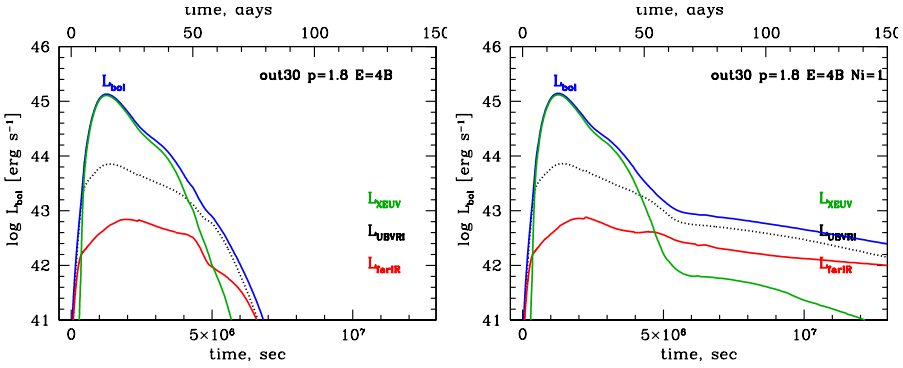


Figure 5 ^{56}Ni vs. shock wave heating. Left: no ^{56}Ni, right: $M(^{56}\mathrm{Ni}) = 1\,M_\odot$ in the ejecta.

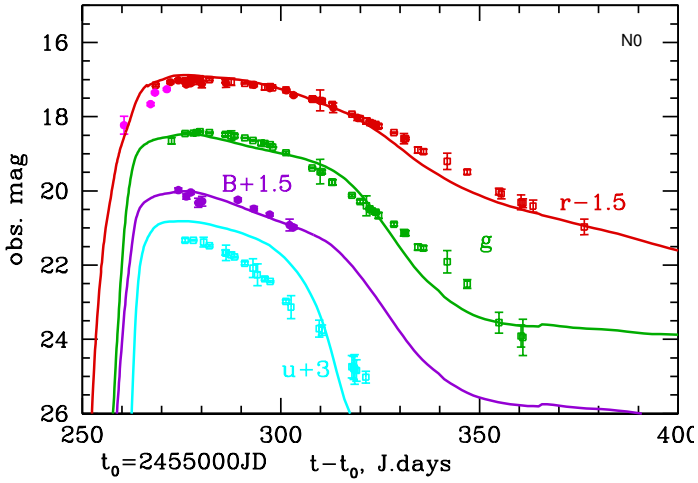


Figure 6 Light curves computed for SN 2010gx.

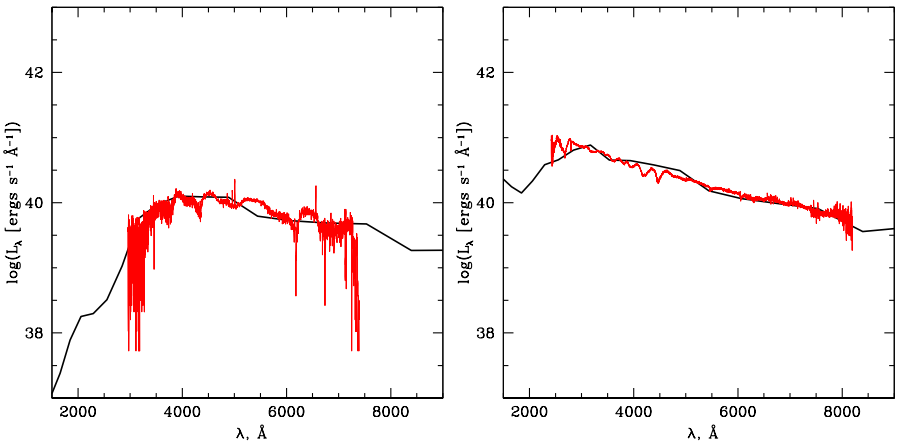


Figure 7 Continuum spectra computed for SN 2010gx (left) and PTF09cnd (right).

4 Now a GRB enters

We have seen that formation of a dense shell is a generic feature of SLSNe. What happens if a GRB explodes inside that shell after the Supernova? Figure 8 from Woosley et al. (2007) shows a possible sequence of events for Pulsational Pair Instability Supernova (PPISN). Two pulses of SN may be followed by a collapse with GRB production (red line on the figure).

The question of GRB interaction with non-uniform interstellar medium was studied in our papers Bad'in et al. (2010); Badjin et al. (2013).

A sketch of GRB-shell interaction is given in Fig. 9.

We have the following sequence of events. A massive star → experiences pulsations or instabilities → this implies 1-st ejection → 2-nd ejection (like in Fig. 8), ejected

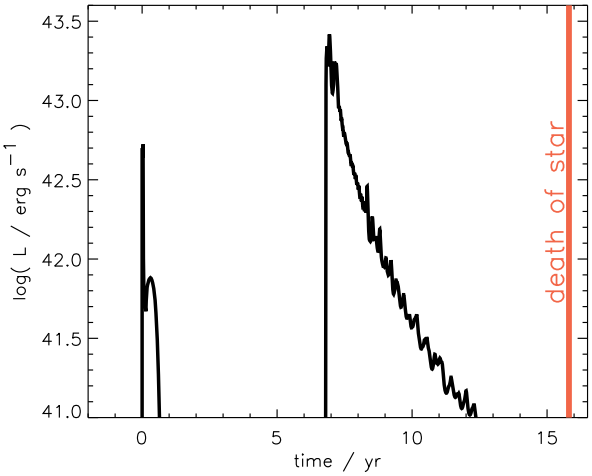


Figure 8 Repeated SN outbursts and final collapse of a star with initial mass ∼110 $M_\odot$ from (Woosley et al., 2007).

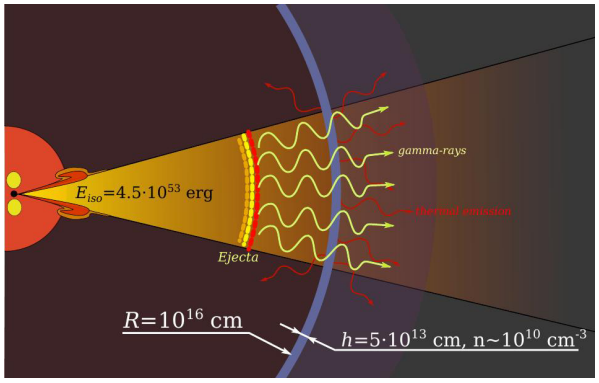


Figure 9 Interaction of GRB emission and its relativistic ejecta with the dense shell from previous SN explosions.

masses collide and form structures (e.g., dense shells discussed above and shown in Fig. 3) → . . . a few years later there is a collapse → GRB, the shell is illuminated by the prompt gamma-emission, and a bit later the relativistic ejecta run into the shell.

The shell is geometrically thin but very massive, ∼5 $M_\odot$. It gains the energy from GRB and should radiate it.

Initial model resembles the supernova shell from Woosley et al. (2007). Abundances were taken from that paper. A continuous spherical shell is discretized with ∼100 concentric mass coordinate layers to be run with a modified version of our STELLA code. The modifications were implemented along the following lines. To treat the interaction of gamma-rays with matter, a time-dependent system of ionization balance equations is solved. Photoionization, ionization due to Compton scattering on bound electrons, collisional ionization, radiative and dielectronic recombination are

taken into account. These processes describe the influence of gamma-rays on the state of plasma, its opacity and emissivity.

Particle density is $n \sim 10^{10}$ cm^{-3} and extents to $r \sim 10^{16}$ cm, while relative thickness of the shell is rather small, $\delta r/r = 0.005$. Thomson optical thickness is not high: $\tau_T \sim 1$. Various configurations have been simulated, but such a 'wall' on the way of GRB emissions displays the most pronounced effects when illuminated by gamma-radiation or heated by the relativistic ejecta plunging into it.

Gamma-ray illumination of the shell was simulated by using Fast Rise and Exponential Decay (FRED) pulses. Three FRED pulses were taken with a time-scale 1.3 s each, duration ∼15 s and isotropic total energy of gamma-ray emission $\approx 4.5 \cdot 10^{53}$ erg. The gamma-ray light curve was intentionally made 'spiky' to see the possible quick response of the surrounding shell to such rapidly altering 'perturbations' (no effect was actually found). A broken power-law spectrum with Band's parameters $\alpha = 0.9, \quad \beta = 2, \quad E_0 = 300$ keV and 100 energy bins were used in the in the range 1 keV–30 MeV. Assumed collimation half opening angle was $\theta_{\rm jet} = 10^\circ$. To treat the emergent thermal emission, 120 frequency groups from 50 000 in IR to 30 keV in X-rays were used.

The opacity of the shell matter should not block the hard emission of relativistic shocks in the GRB ejecta (in order to allow observation of the GRB phenomenon itself). This requirement is fulfilled because the matter is quickly ionized by gamma-rays. Thus, both the prompt non-thermal GRB emission and the early X-ray afterglow will be visible until the recombination of matter occurs. At the same time the ionization and excitation of plasma makes it opaque to the visible light.

The radiative heating of cold matter is produced by the gamma-ray radiation via photoionization and Compton scattering (with opacity coefficients depending on the non-stationarily calculated state). In addition to the heating effect, the radiation drag force produced by gamma-radiation is taken into account.

As the radiation front moves with the speed of light, the unheated regions are not causally connected to heated ones; there is a sharp discontinuity in temperature, ionization, opacity and emissivity behind the gamma-ray front. No outward fluxes of heat, mass and radiation through this contact discontinuity are assumed as boundary conditions. In the modified code this is taken into account. When calculating the Eddington factors of the thermal emission (see Blinnikov et al. 1998), the heated and unheated parts of the shell are treated independently.

We place the inner boundary flux condition by means of the inner boundary Eddington factors. They are calculated similarly to those at the outer boundary in the original STELLA code ($\mathcal{H}_\nu = h_{\rm E}\mathcal{J}_\nu$ in terms of Blinnikov et al. 1998). An arbitrary incoming boundary flux, e.g. a diluted blackbody background or a counter-jet emission, can also be taken into account.

In addition to being heated by gamma-rays, the shell is heated due to partial thermalization of the GRB jet kinetic energy. Clearly, the one-dimensional non-relativistic code cannot model the relativistic jet dynamics self-consistently; therefore we model the jet impact by means of a 'thermal bomb'. In this approach, which is widely used in simulations of supernovae, the jet braking and its kinetic energy dissipation are described in terms of the thermal energy which is deposited into selected zones during the time interval mostly appropriate for the effective dissipation process.

This general approach is rather insensitive to details of the GRB fireball expansion

or blast wave propagation. Assuming energy equipartition between the gamma-rays and ejecta, we have taken 4.5×10^{53} erg as an estimate of the energy to be thermalized. In fact, results of calculations turned out to be sensitive to the total thermalized energy and weakly depend on deviations from the equipartition.

The impact of GRB Ejecta on the shell was described in simulations in the following way.

Immediate deceleration is assumed for the mass $M_{\rm dec}$ within the limits

$$\frac{E_k}{c^2\Gamma} \le M_{\rm dec} < \frac{E_k}{c^2\Gamma^2} << M_{\rm shell},$$

Hence thermalization of the energy E_k.
Thermal energy $E_k = E_{{\rm iso},\gamma} = 4.5\cdot10^{53}$ erg is deposited into the innermost zone over $\delta R_z/c \approx 17$ s time scale.
The 'thermal bomb' is triggered with the burst time

$$\Delta t_{\gamma-ej} \sim \frac{R}{2c\Gamma^2} \approx 200 \quad \text{seconds}$$

for $\Gamma = 30$. A clumpy structure is necessary to let the long-term synchrotron afterglow to be emitted.

Thermal emission modelling assumed the following.

- $O(v/c)$ aberration, Doppler shift, retardation; 120 groups from infrared 50000 Å up to 100 keV X-ray.
- Emission coefficient $\eta_\nu = \chi_{ab} b_\nu$, where b_ν is blackbody intensity, and absorption coefficient χ_{ab} contains free-free, bound-free, and lots of bound-bound processes (i.e. spectral lines), plus account of the expansion opacity effect like in STELLA.
- Boundary conditions for the Eddington flux $\mathcal{H}_\nu$ expressed through the zero moment of intensity $\mathcal{J}_\nu$:
$$\mathcal{H}_\nu = h_E \mathcal{J}_\nu.$$
On the outer boundary the thermal flux is positive $\mathcal{H}_\nu > 0$; on the inner boundary it is negative $\mathcal{H}_\nu < 0$. Pressure $P_{\rm out} = 0$.
- Light travel time correction was taken into account:
$$L_{\nu,{\rm iso}}(t_{\rm obs}) = 8\pi^2 \int\limits_{\mu_{min}}^{1} \mu I_\nu(t'_{\rm del},\mu) R^2_{\rm out}(t'_{\rm del}) {\rm d}\mu,$$
where $t'_{\rm del} + \frac{R_{\rm out}(t'_{\rm del})}{c}(1-\mu) = t_{\rm obs}$.

The resulting light curves are presented in our paper Badjin et al. (2013). The most prominent displays of thermal effects in visible light should be looked for in high-redshift objects' light curves. The fluxes in R-band can be very high within few hours and first days after the GRB, see Fig. 10.

Optical afterglows of several GRBs demonstrate clear deviations from the pure power-law decay (see e.g. discussion in Bad'in et al. 2010). These 'bumps' correspond

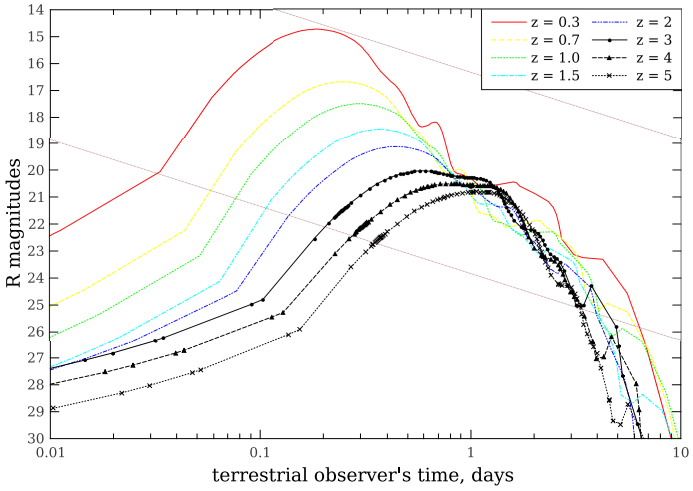


Figure 10 Calculated R-fluxes of thermal emission seen from different redshifts. The straight dotted lines show the characteristic range of the observed R-band afterglows of GRBs. From (Badjin et al., 2013).

to additional proper luminosities of the order of 10^{43}–10^{45} erg s^{-1}, which is close to what is expected from thermal emission of circumburst shells illuminated by prompt GRB emission. The qualitative agreement with observations of GRB 021004, located at $z \approx 3$ is shown in Fig. 11.

Due to high densities and radiation fluxes (both thermal and non-thermal), the radiation pressure can dominate the gas pressure by four orders of magnitude. This makes the problem very sensitive to the local opacity, to direction and strength of

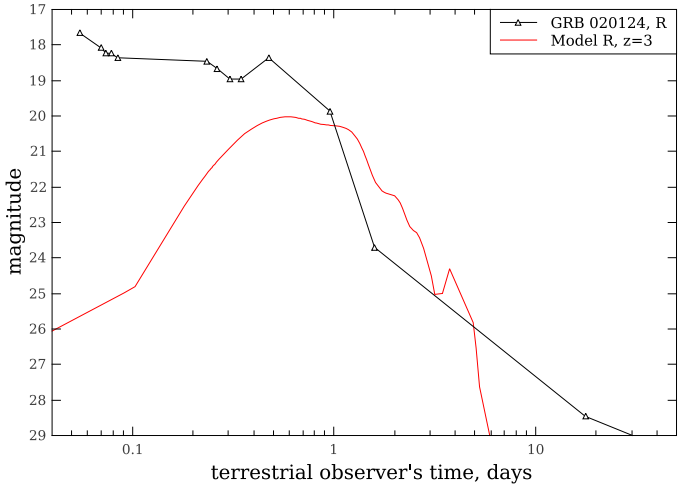


Figure 11 The GRB 020124 optical afterglow in the R band (open circles) and the $z = 3$ calculated thermal emission R-band stellar magnitudes (solid line).

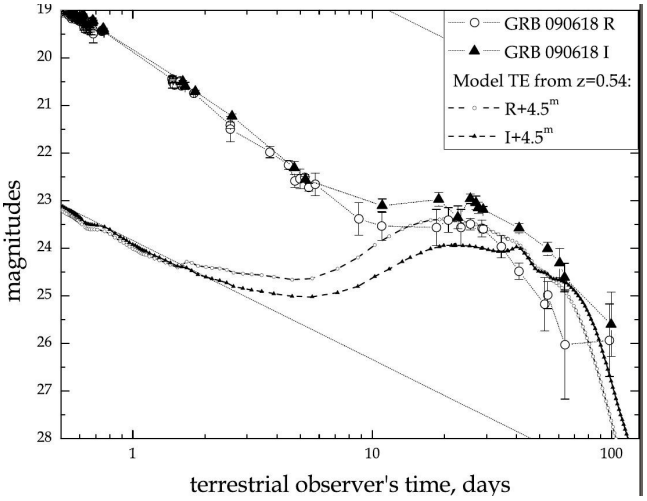


Figure 12 Comparison of QSN simulations with observations of GRB060218.

radiation flows. Depending on whether there are highly opaque regions (where the radiation is strongly coupled with matter) or how transparent the inner boundary is, the radiation either flows away, exhausting shell's thermal energy, or is accumulated in hot regions and drives their expansion.

The latter, for example, takes place if the inner boundary for some reason does not transmit the soft radiation towards the centre (e.g. the layers at this boundary are highly compressed by the shock and rather opaque, or they scatter the radiation back, or relativistic aberration forces most of the emission to flow outwards). Then the thermal radiation appears trapped between the 'no-flux-towards-the-centre' inner and 'no flux outwards' intermediate boundaries, accelerating the hot zones rapidly up to several 10^4 km s^{-1}, which results in a 'quasi-supernova' (QSN) event. As matter is needed to be compressed by several orders of magnitude to compensate the radiation pressure, a radiation-driven implosion easily develops around the opacity jumps or radiation flux jumps. The compression leads to the growth of opacity, providing a positive feedback on the implosion, until the radiative pressure growth coasts or possible instabilities come into play smearing off the density peak.

Let us consider an extreme case: inner boundary completely reflecting the inward flux, $\mathcal{H}_{\nu,in} = 0$. In this case the simulations predict the following features.

Total peak luminosity $\sim 10^{49}$ erg/s, X-rays are unaffected since they depend mostly on gamma-rays. In visible light: **a bright flash** (like a shock breakout) $\rightarrow$ **a long bump/plateau**.
Expansion velocity $\sim 6.5 \cdot 10^4$ km/s. It looks like a very energetic supernova.
Double-bumped light curves are predicted (Badjin et al., 2013) and similar features are reported for GRB 060218 (SN 2006aj) by Campana et al. (2006), see Fig. 12. An X-ray blackbody component is also reported with a plateau of $\geq$3000 s duration.
QSN modelling is non-physical in 1D, but it illustrates **the importance of radiation** around an opacity jump (this may be natural in 2D or 3D cases, near surfaces dividing hot and cold dense matter, e.g. at jet channel walls). **A curious consequence** for

the GRB-SN connection and central engine theory: since the SN-bump is allowed to originate in the environment (here it is due to an explosion driven by radiation), **it removes the necessity for the central engine of the collimated 'failed supernova' outflow, to launch a 'successful' SN as well.** The latter occurs outside.

A combination of ideas of the 'failed supernova' by Woosley (1993), and 'supranova' by Vietri and Stella (1998, 1999), emerges.

5 Conclusions

The shock wave which runs through rather dense matter surrounding an exploding star can produce enough light to explain very luminous SN events, SLSNe. No ^{56}Ni is needed in this case to explain the light curve near maximum light (some amount may be needed to explain light curve tails). We need the explosion energy of only 2–4 Bethe for the shell with $M = 3$–$6\ M_\odot$ and $R \lesssim 10^{16}$ cm. Narrow lines are not necessarily produced, since the first ejection could produce fast moving matter. However, in this case it is hard to obtain a very long light curve, so ^{56}Ni or another kind of energy pumping for the tail is needed.

The peak power and the duration of the light curve maximum depend strongly on the mass, structure and on the explosion energy. The features of monochromatic light curves sometimes depend on chemical composition of the envelope.

Questions on the latest phases of star evolution arise:

- Is it possible to form so big and dense envelopes? And how?
- Time scale for such a formation
- How far can the envelope extend?
- Density and temperature profiles inside the envelope right before the explosion

There are also questions to observations: one should try to find traces of such shells for the bright explosions. (There is spectral evidence of circumstellar shells for type IIn and Ibn SNe. Is it possible to find C–O envelopes as well?)

Important conclusions may be drawn also on Thermal Emission in GRB afterglows.

- Massive structures of circumstellar matter must produce **detectable Thermal Emission**, plateaus, bumps, irregularities in GRB afterglows.
- A possibility of off-centre supernova-like explosions $\Rightarrow$ **a way to explain the GRB-SN connection** without placing constraints on GRB central engine.
- An important role of radiation implies a necessity in self-consistent relativistic multidimensional **Radiation** hydrodynamics codes.

For both classes of problems considered in this report one has to solve many technical problems in light curve calculations, e.g:

- line opacities;
- dimensionality: 3D is preferable, since the envelope can most probably be clumpy;
- NLTE spectra.

Acknowledgements

Our work is supported by a grant of Russian Science Foundation 14-12-00203.

References

Baklanov, P. V., Blinnikov, S. I., & Pavlyuk, N. N. 2005, Astronomy Letters, 31, 429
Barkov, M. V., & Komissarov, S. S. 2011, MNRAS, 415, 944
Blinnikov, S. I., Eastman, R., Bartunov, O. S., Popolitov, V. A., & Woosley, S. E. 1998, Astroph. J., 496, 454
Blinnikov, S. I., Röpke, F. K., Sorokina, E. I., et al. 2006, Astron. Ap., 453, 229
Chevalier, R. A. 2012, Astroph. J. Lett., 752, L2
Chugai, N. N., Blinnikov, S. I., Cumming, R. J., et al. 2004, MNRAS, 352, 1213
Grasberg, E. K., & Nadyozhin, D. K. 1986, Soviet Astronomy Letters, 12, 68
Heger, A., & Woosley, S. E. 2002, Astroph. J., 567, 532
Quimby, R. M., Yuan, F., Akerlof, C., & Wheeler, J. C. 2013, MNRAS, 431, 912
Sorokina, E., Blinnikov, S., Nomoto, K., Quimby, R., Tolstov, A. 2015. Type I Superluminous Supernovae as Explosions inside Non-Hydrogen Circumstellar Envelopes. ArXiv e-prints arXiv:1510.00834
Woosley, S. E., Blinnikov, S., & Heger, A. 2007, Nature, 450, 390
Badjin, D. A., Blinnikov, S. I., Postnov, K. A. 2013. Thermal emission in gamma-ray burst afterglows. Monthly Notices of the Royal Astronomical Society 432, 2454-2462
Bad'in, D. A., Blinnikov, S. I., Postnov, K. A. 2010. Heating of the circumstellar medium by gamma-ray burst prompt emission. Astronomy Letters 36, 687–706
R.K. Brayton, F.G. Gustavson and G.D. Hatchel, A new efficient algorithm for solving differential- algebraic systems using implicit backward differentiation formulas, Proc. IEEE 60 (1) (1972) 988108
M.M. Stabrowski. 1997. An efficient algorithm for solving stiff ordinary differential equations, Simulation Practice and Theory, 5(4), 333
Campana S. et al., 2006, Nat, 442, 1008
Woosley S.E., 1993, ApJ, 405, 273
Vietri, M., Stella, L. 1999. Supranova Events from Spun-up Neutron Stars: An Explosion in Search of an Observation. The Astrophysical Journal 527, L43–L46
Vietri, M., Stella, L. 1998. A Gamma-Ray Burst Model with Small Baryon Contamination. The Astrophysical Journal 507, L45–L48